THE JOURNAL OF BIOLOGICAL CHEMISTRY
Vol. 279, No. 17, Issue of April 23, pp. 17338–17347, 2004

Printed in U.S.A.

Development of Protein-based Inhibitors of the Proprotein of Convertase SKI-1/S1P

PROCESSING OF SREBP-2, ATF6, AND A VIRAL GLYCOPROTEIN*

Received for publication, December 16, 2003, and in revised form, January 20, 2004
Published, JBC Papers in Press, February 16, 2004, DOI 10.1074/jbc.M313764200

Philomena Pullikotil‡, Martin Vincent§, Stuart T. Nichol§, and Nabil G. Seidah‡¶

From the ‡Laboratories of Biochemical Neuroendocrinology, Clinical Research Institute of Montreal, Montreal, Quebec H2W 1R7, Canada and the §Special Pathogens Branch, Division of Viral and Rickettsial Diseases, Centers for Disease Control and Prevention, Atlanta, Georgia 30333

Processing of membrane-bound transcription factors such as sterol regulatory element-binding proteins (SREBPs) and the ER-stress response factor ATF6, and glycoproteins of some hemorrhagic fever viruses are initiated by the proprotein convertase SKI-1/S1P. So far, no cellular protein-based inhibitor of the hydrophobic-amino acid specific SKI-1 is known. The prosegment of the basic-amino acid specific convertases (*e.g.* furin and PC5) or α_1-PDX, a variant of α_1-antitrypsin (α_1-AT) exhibiting an RIPR^{358} sequence at the reactive site loop, were shown to potently inhibit these secretory proteinases. Accordingly, we tested the SKI-1-inhibitory potential of various point mutants of either the 198 amino acid preprosegment of SKI-1-(1–198) or α_1-AT. Transient transfections data showed that, out of numerous mutants studied, the R134E prosegment mutant or the α_1-AT reactive site loop variants RRVL^{358}, RRYL^{358} and RRIL^{358} are the best specific cellular inhibitors of SKI-1. The observed inhibition of the processing of endogenous SREBP-2, exogenous ATF6 and a PDGF-A (RRLL^{86}) variant were >55% and reach ~80% in stable transfectants. We also show that SKI-1 forms SDS-stable complexes with these α_1-AT variants, but not with wild-type α_1-AT or α_1-PDX. Finally, these inhibitors were also shown to affect the processing and stability of the Crimean-Congo hemorrhagic fever virus glycoprotein.

Proteins and peptides that are biologically active are often generated by intracellular limited proteolysis of inactive precursors. The mammalian proprotein convertases (PCs)[1] of the secretory pathway are calcium-dependent serine proteinases related to bacterial subtilisin that cleave various precursors at the general consensus motif (K/R)(X)$_n$(K/R)↓, where n = 0, 2, 4, or 6 and X is any amino acid (1–3). The PC family counts seven basic amino acid-specific kexin-like convertases: furin, PC1/3, PC2, PC4, PACE4, PC5/6, and PC7/LPC (4). The eighth member is the recently discovered pyrolysin-like SKI-1/S1P that cleaves at the consensus motif (R/K)X(hydrophobic)Z↓, where Z is variable (5), while the last member (6, 7) NARC-1 cleaves the sequence VFAQ^{153}↓ in its prosegment (8, 9).[2]

More PCs contain an N-terminal signal sequence, followed by a prosegment, a catalytic domain and a P-domain. In addition, PCs possess a C-terminal segment that varies between the different members. The critical role of PCs in the proteolytic maturation of multiple proproteins, their implication in various pathologies (1, 10, 11), and their unidentified specific and/or redundant functions, make them attractive targets for the development of potent and selective inhibitors. The various successful approaches include: active site-directed chloromethyl ketone inhibitors (12, 13), reversible peptide-based inhibitors (14–17), plant derivatives (18), and several engineered variants of protein-based inhibitors that possess a furin-like motif. These include α2-macroglobulin (α2-MF) (19), α_1-antitrypsin (α_1-AT) Portland (α_1-PDX) (20–22), proteinase inhibitor 8 (PI8) (23), the turkey ovomucoid third domain (24), and eglin C (25, 26). However, these effective inhibitors directed against the basic amino acid-specific members lack selectivity. Furthermore, α_1-PDX was shown to inhibit all the basic amino acid-specific PCs within the constitutive secretory pathway (21, 27), whereas PI8 and α2-MF can inhibit many other proteases in addition to the PCs.

Subtilisin-, kexin-, and furin-based studies established that the prosegment of these enzymes could act both as an intramolecular chaperone and a potent inhibitor (28–31). The prodomain of PCs acts as a competitive inhibitor (31–34), whereas the prodomain of the yeast kexin behaves as a mixed inhibitor with an IC_{50} of ~160 nM (29). The wild-type prosegment of SKI-1 was also shown to inhibit this enzyme *in vitro*, albeit at micromolar concentrations (35). Finally, it was shown that *ex vivo* overexpression of the preproregions of furin (ppfurin), PC7 (ppPC7), and PC5 (ppPC5) resulted in potent but moderately selective cellular inhibition of their parent enzyme (31, 33, 36).

* This work was supported by a Canadian Institutes of Health Research (CIHR) Grant MOP-36496, and by the Protein Engineering Network of Excellence (PENCE). The costs of publication of this article were defrayed in part by the payment of page charges. This article must therefore be hereby marked "*advertisement*" in accordance with 18 U.S.C. Section 1734 solely to indicate this fact.

¶ To whom correspondence should be addressed: Laboratory of Biochemical Neuroendocrinology, Clinical Research Institute of Montreal, 110 Pine Ave. West Montreal, QC H2W 1R7 Canada. Tel.: 514-987-5609; Fax: 514-987-5542; E-mail: seidahn@ircm.qc.ca.

[1] The abbreviations used are: PC, proprotein convertase; SKI-1, subtilisin kexin isozyme-1; ppSKI-1, preprosegment of SKI-1 enzyme; S1P, site-1-protease; pro-PDGF, precursor of platelet-derived growth factor; ER, endoplasmic reticulum; CHO, Chinese hamster ovary; WT, wild type; EGFP, enhanced green fluorescent protein; SCAP, sterol cleavage-activating protein; SREBP, sterol regulatory element-binding protein; nSREBP, nuclear SREBP; ATF6, activating transcription factor 6; CCHF, Crimean Congo hemorrhagic fever; AEBSF, 4-(2-aminoethyl)-benzenesulfonyl fluoride; ALLN, N-acetyl-leucinal-leucinal-norleucinal; α_1-AT, α_1-antitrypsin; α_1-PDX, α_1-antitrypsin Portland; UPR, unfolded protein response; RSL, reactive site loop; PBS, phosphate-buffered saline; PDGF, platelet-derived growth factor; DMEM, Dulbecco's modified Eagle's medium; HMAF, hyperimmune mouse ascites fluid.

[2] S. Benjannet, L. Wickham, D. Rhainds, J. Mayne, M.-C. Asselin, J. Hamelin, M. Varret, D. Allard, M. Abifadel, C. Boileau, A. D. Attie, M. Chretien, A. Prat, and N. G. Seidah, submitted for publication.

Subtilisin kexin isozyme-1 (SKI-1) (5, 7) also known as Site 1 protease (6) represents the first mammalian member of secretory subtilisin-like processing enzymes that cleaves after hydrophobic residues. It is synthesized as an inactive precursor (1,052 amino acids) that undergoes three sequential autocatalytic processing events of its prosegment (amino acids 17–186). The signal peptidase cleavage generates an A form (amino acids 17–1052) that is subsequently autocatalytically cleaved in the endoplasmic reticulum (ER) at two alternate B′ and B sites: $RKVF^{133}\downarrow$ (SKI-1-(134–1052)) and $RKVFRSLK^{137}\downarrow$ (SKI-1-(138–1052)), respectively. The latter products are then transported to the *cis/medial* Golgi whereupon they are further autocatalytically processed into a C-form at $RRLL^{186}\downarrow$, generating SKI-1-(187–1052) (5, 7, 35, 37).

SKI-1 plays a crucial role in the regulation of lipid metabolism and cholesterol homeostasis through the processing of the sterol regulatory element-binding proteins, SREBP-1 and SREBP-2, which occurs in the *cis/medial* Golgi (38, 39). Other type-II membrane-bound substrates include ATF6 that plays a major role in the unfolded protein response (UPR) to enhance the protein folding or refolding capacity of the secretory pathway (40, 41), and the basic leucine zipper transcription factor Luman, the cellular counterpart of herpes simplex virus VP16 (42). Brain-derived neurotrophic factor (BDNF) is a soluble substrate and the study of its processing led to the initial cloning of SKI-1 (5). Mutation of proplatelet-derived growth factor A (pro-PDGF-A) at its furin-cleavage site ($RRKR^{86}$) into $RRLL^{86}$ (pro-PDGF-A*) resulted in a SKI-1 artificial substrate (43). Finally, SKI-1 was shown to play a major role in the processing of surface glycoproteins of infectious viruses such as Lassa (44, 45), lymphocytic choriomeningitis (LCMV) (46, 47) and Crimean Congo hemorrhagic fever (CCHF) (48) viruses. CCHF is a tick-borne member of the genus *Nairovirus*, family Bunyaviridae. The mature virus glycoprotein Gn is generated by proteolytic cleavage from Pre-Gn at the RRLL site by SKI-1 in the ER-*cis* Golgi compartments (48).

The three SREBP isoforms in mammals that belong to the basic helix-loop-helix leucine zipper (bHLH-Zip) family of transcription factors are designated SREBP-1a, SREBP-1c, and SREBP-2 (39). Synthesized as membrane-bound precursors, they are cleaved in an SREBP-cleavage-activating protein (SCAP)- and insulin-induced gene (Insig)-dependent fashion. When cellular cholesterol levels are high, Insig proteins bind and retain the SCAP-SREBP complex in the ER. When cells are deprived of sterols, Insig separates, allowing the transport of the SREBP-SCAP complex to the Golgi. Therein, a two-step proteolytic process (SKI-1/S1P and S2P) (49), releases the SREBPs from cell membranes, allowing their active N-terminal segments (nSREBP) to translocate to the nucleus, where they activate transcription of more than 25 mRNAs coding for proteins required for the biosynthesis and uptake of cholesterol and unsaturated fatty acids (50).

ATF6 is an ER type II leucine zipper transmembrane transcription factor held in the ER by Bip under normal conditions, with its N-terminal DNA binding domain facing the cytosol and its C terminus in the ER lumen (51). Accumulation of improperly folded proteins in the ER, calcium depletion by thapsigargin or inhibition of glycosylation by tunicamycin leads to an ER-stress response resulting in Bip dissociation from ATF6. The latter is then translocated in a SCAP-independent fashion to the Golgi where it is first cleaved by SKI-1/S1P and then by S2P. This releases the cytosolic N-terminal domain of ATF6 (nATF6), which subsequently reaches the nucleus to activate ER stress target genes (41, 52).

SREBPs and their processing enzymes, SKI-1/S1P and S2P are certainly important targets for drug development. A sensitive SKI-1-specific fluorogenic assay has been developed based on the processing of a quenched fluorogenic peptide mimicking the glycoprotein processing site of Lassa (45) and CCHF (48) viruses. It was shown *in vivo* that SKI-1/S1P plays a crucial role in the processing of SREBPs in liver and is necessary for normal rates of triglyceride and sterol synthesis. Thus, whereas homozygote SKI-1/S1P (−/−) results in a lethal phenotype, conditional knockout in mouse liver results in 64–83% decrease in the rates of cholesterol and fatty acid biosynthesis in hepatocytes (53). However, analysis of SKI-1 mRNA distribution revealed a widespread expression that suggests that this convertase plays other roles, as in neurons, bone and cartilage development (5). Indeed, it was recently shown that SKI-1 plays a critical role in cartilage development in zebrafish (54).

The critical implication of SKI-1 in various cellular functions and in certain pathologies emphasizes the importance of understanding the function of this convertase and of developing specific inhibitors that could modulate its activity in disease states. Whereas SKI-1 inhibition was recently achieved with 300 μM of the general serine protease inhibitor AEBSF (55), it was not a specific SKI-1 inhibitor. In the present study, we introduced SKI-1 recognition motifs into the reactive site loop (RSL) of α_1-AT (P1-P4 positions) as one approach to the development of protein-based inhibitors. We also optimized the prosegment-based inhibition of SKI-1 and identified a unique R134E mutant exhibiting a potent inhibitory activity. These inhibitors represent protein-based inhibitors designed to specifically block intracellular SKI-1 activity.

EXPERIMENTAL PROCEDURES

Construction of Human α_1-AT Variants by Site-directed Mutagenesis—The pIRES2-EGFP vector (Clontech) with the human α_1-AT cDNA containing the wild-type sequence ($AIPM^{358}$) in the reactive site loop (RSL) was used as template to introduce mutations. The various P1-P4 reactive site loop variants were generated by a two-step PCR using Elongase (Invitrogen, Life Technologies) using sense (S) and antisense (AS) oligonucleotides. The oligonucleotides used for introducing mutants were S1/AS1, S2/AS2, S3/AS3, S4/AS4, S5/AS5, and S6/AS6, S7/AS7, S8/AS8, S9/AS9, S10/AS10, S11/AS11, and S12/AS12, respectively (Table I). The various α_1-AT variants were subsequently amplified using S22/AS22, and the PCR products were cloned into the pCRII-TOPO TA-cloning vector (Invitrogen) and sequenced. The PstI/SacII cDNA fragments replaced that of the wild-type α_1-AT sequence in the pIRES2-EGFP, resulting in the mutant α_1-AT recombinants RRLL, RSLK, RRLI, RRLV, RKVF, RRLE, RRIL, RRVL, RRFL, RRYL, KRLL, and KKLL.

Human Prepro-SKI-1 and Its Mutants—The N-terminal fragment of hSKI-1 (wild type) (1–198 amino acids) was amplified by PCR using S13/AS13 and cloned into pCRII-TOPO TA-cloning vector. Subsequently, the amplified cDNA was digested by XhoI/BamHI and subcloned into pIRES2-EGFP. Site-directed mutagenesis was carried out using the wild-type construct as the template using the pairs of oligonucleotides (Table I): S13/AS14, S15/AS15, S16/AS16, S17/AS17, S18/AS18, S19/AS19, S13/AS20, S21/AS21. This generated the preproSKI-1 (ppSKI-1) cleavage B′/B site mutants $RKVFRSLK^{137}$-stop, R134E, R134A, K137V, K131A, R130A (amino acids 1–198)-KDEL, and the double mutant K130A/R131A. All mutant cDNAs were sequenced and subcloned into pIRES2-EGFP.

Inhibition of Pro-PDGF-A and Pro-PDGF-A Processing ex Vivo*—Chinese hamster ovary CHO-K1 (4×10^5) cells (in a 60-mm plate) were transfected using LipofectAMINE 2000 (Invitrogen). A total of 6 μg of DNA was used for each transfection in a ratio of 1:4 (substrate:inhibitor) expressing either pIRES2-EGFP-V5 alone, pIRES2-EGFP-pro-PDGF-A-V5 (WT), or pIRES2-EGFP-pro-PDGF-A*-V5 (mutant). Co-transfection with various mutants constructs such as α_1-PDX ($RIPR^{358}$), α_1-AT ($AIPM^{358}$) WT, various α_1-AT, and ppSKI-1 variants were used to inhibit the processing of wild-type pro-PDGF-A or its $RRLL^{86}$ mutant (pro-PDGF-A*). After 24 h of incubation at 37 °C in DMEM/10% fetal calf serum (Invitrogen, Life Technologies), the cells were rinsed with PBS and incubated in serum-free DMEM for another 24 h. 48-h post-transfection, the medium was resolved on a 12% SDS-PAGE gel. Detection by Western blotting was done with monoclonal

TABLE I
Oligonucleotides Sense (S) and Antisense (AS) used in the construction of various α_1-AT and ppSKI-1 mutants

Primers	Sense (S)	Antisense (AS)
S1/AS1	CGCAGACTCCTCTCGATCCCCCCCGAGGTCAAG	GAGGAGTCTGCGCTCTAAAAACATGGCCCCTGC
S2/AS2	CGCAGTCTCAAATCGATCCCCCCCGAGGTCAAG	TTTGAGACTGCGCTCTAAAAACATGGCCCCTGC
S3/AS3	CGCAGACTCATCTCGATCCCCCCCGAGGTCAAG	GATGAGTCTGCGCTCTAAAAACATGGCCCCTGC
S4/AS4	CGCAGACTCGTCTCGATCCCCCCCGAGGTCAAG	GACGAGTCTGCGCTCTAAAAACATGGCCCCTGC
S5/AS5	CGCAAAGTCTTCTCGATCCCCCCCGAGGTCAAG	GAAGACTTTGCGCTCTAAAAACATGGCCCCTGC
S6/AS6	CGCAGACTCGAGTCGATCCC	GGGATCGACTCGAGTCTGCG
S7/AS7	GAGCGCAGAATCCTCTCGATCC	GGATCGAGAGGATTCTGCGCTC
S8/AS8	GAGCGCAGAGTCCTCTCGATCC	GGATCGAGAGGACTCTGCGCTC
S9/AS9	GAGCGCAGATTCCTCTCGATCC	GGATCGAGAGGAATCTGCGCTC
S10/AS10	GAGCGCAGATACCTCTCGATCC	GGATCGAGAGGTATCTGCGCTC
S11/AS11	GTTTTTAGAGAAGAGACTCCTCTCG	CGAGAGGAGTCTCTTCTCTAAAAAC
S12/AS12	GTTTTAGAGAAGAAACTCCTCTCG	CGAGAGGAGTTTCTTCTCTAAAAAC
S13/AS13	GGATCCGAAGAAACATCTGGGCGACAGA	CTCGAGTGTCTGGGCAACCTGGCGCGGG
S13/AS14	GGATCCGAAGAAACATCTGGGCGACAGA	ATGGATCCCTATTCAGCATACTTGAGGGAACG
S15/AS15	GAAAAGTCTTTGAATCCCTCAAG	CTTGAGGGATTCAAAGACTTTTC
S16/AS16	GAAAAGTCTTTGCTTCCCTCAAG	CTTGAGGGAAGCAAAGACTTTTC
S17AS17	GTTCCCTCGTGTATGCTGAATCTG	CAGATTCAGCATACACGAGGGAAC
S18/AS18	CCCCAACGTGCAGTCTTCCGTTCC	GGAACGGAAGACTGCACGTTGGGG
S19/AS19	CCCCAAGCGAAAGTCTTCCGTTCC	GGAACGGAAGACTTTCGCTTGGGG
S13/AS20	GGATCCGAAGAAACATCTGGGCGACAGA	GGATCCTCACAGTTCATCTTTCTGCAGTGT CTGGGCAACCTG
S21/AS21	CCCCAAGCAGCTGTCTTTCGTTCC	GGAACGAAAGACAGCTGCTTGGGG
S22/AS22	CTCACCCACGATATCATCACC	CTTCGGCCAGTAACGTTAGGGG

antibody directed against the V5 epitope fused to the C-terminal end of pro-PDGF-A (1:5000 dilution) (Invitrogen).

Transient Transfection and Immunoblot Analysis of Endogenous Hamster SREBP-2—Chinese hamster ovary cells (CHO-K1) were set up at a density of 4×10^5 cells per 60-mm plate for transfection. On day 1, cells were transiently transfected with 6 μg of cDNA using LipofectAMINE 2000, and cultured overnight in medium B (1:1 mixture of Ham's F-12 medium and Dulbecco's modified Eagle's medium containing 100 μg/ml streptomycin sulfate) supplemented with 5% fetal calf serum. On day 2, cells were washed with PBS and then switched to medium with 5% lipoprotein deficient serum (LPDS) with 50 μM compactin and 50 μM sodium mevalonate in the absence or the presence of sterols for 18 h. Thereafter, the cells received *N*-acetyl-leucinal-leucinal-norleucinal (ALLN; Sigma) at a final concentration of 25 μg/ml, a calpain and proteasome inhibitor that blocks the degradation of the mature form of SREBP-2, and the cells harvested 1-h later. Cells were then washed twice with PBS, lysed in 200 μl of SDS buffer (10 mM Tris, pH 7.5, 100 mM NaCl, 1% SDS, and 25 μg/ml ALLN), passed repeatedly through a 25-gauge needle, and centrifuged. Cell lysates were separated by electrophoresis on 6% SDS-polyacrylamide gel and the separated proteins were transferred to Hybond-C nitrocellulose membranes (Amersham Biosciences). These were then incubated with a mouse monoclonal antibody IgG-7D4 (dilution 1:200) directed against the N-terminal domain of hamster SREBP-2 (amino acids 32–250). The membranes were washed, and the immunoreactive proteins detected with horseradish peroxidase-conjugated anti-mouse IgG using an enhanced chemiluminescence (ECL) Western blotting detection system kit (Amersham Biosciences) according to the manufacturer's instructions.

Inhibitory Effect of Various Mutants on the Processing of ATF6—Monolayers of CHO-K1 cells were set up (4×10^5 cells/60-mm plate) and cultured in (1:1 mixture of Ham's F-12 medium and Dulbecco's modified Eagle's medium containing 100 units/ml penicillin and 100 μg/ml streptomycin sulfate) supplemented with 5% fetal calf serum. The cells were co-transfected with a total of 6 μg of DNA in a ratio of (1:4 substrate: inhibitor). With 3× FLAG-ATF6 and mutant cDNA constructs using LipofectAMINE 2000. Two days post-transfection cells received a direct addition of 25 μg/ml ALLN in the absence or presence of 2 μg/ml tunicamycin (4 h) or 300 nM thapsigargin (1 h). Cells were then washed twice with PBS, lysed in 200 μl of SDS buffer, passed 15–20× through a 25-gauge needle, and centrifuged. The lysates were analyzed by immunoblotting using a 1:5000 dilution of anti-FLAG M2 monoclonal antibody (Stratagene). Horseradish peroxidase-conjugated goat anti-mouse IgG was used as secondary antibody at a 1:10,000 dilution, and the signal was visualized by the ECL chemiluminescence kit.

Formation of Enzyme/Inhibitor Complex in SRD-12B SKI$^{(-)}$ and HK293 Cells—The ability of the serpin-serine proteinase interaction to form SDS- and heat-stable complexes was analyzed by transfecting SRD-12B SKI-1$^{(-)}$ (56) and HK293 cells. SRD12B cells were plated on day 0, (4×10^5 cells) in medium B (1:1 mixture of Ham's F-12 medium and Dulbecco's modified Eagle's medium containing 100 μg/ml streptomycin sulfate supplemented with 5% fetal calf serum, 5 μg/ml cholesterol, 1 mM sodium mevalonate, and 20 μM sodium oleate). The cells were co-transfected with 2 μg of hSKI-V5, SKI-H249A (active site mutant) and 4 μg of various α_1-AT variants constructs, using LipofectAMINE 2000. Human embryonic kidney (HK293) cells (35-mm plate) were co-transfected with 0.8 μg of cDNA expressing SKI-1-V5 or PC5A-V5 and 1.2 μg of various α_1-AT variants using Effectene transfection reagent (Qiagen). 24-h post-transfection, cells were washed with PBS and incubated in serum-free medium for an additional 24 h. 48-h post-transfection SRD-12B SKI-1$^{(-)}$ or HK293 cells were washed with ice-cold PBS and then lysed in 1× radioimmune precipitation assay buffer, proteins were resolved on 6% SDS-PAGE, cell lysate immunoblotted with V5 1:5000 monoclonal antibody.

CCHF Virus Pre-Gn to Gn Processing and Inhibition—SW13 cells were maintained in DMEM supplemented with 10% fetal calf serum. SW13 cells stably expressing α_1-PDX and RRVL^{358} were developed and maintained in the presence of G418 (300 μg/ml). CHO-K1 derived cells expressing α_1-AT, RRVL^{358}, RRYL^{358}, and R134E were maintained in 1:1 proportion of DMEM and Ham's F-12 medium supplemented with 5% fetal calf serum. Hyperimmune mouse ascites fluid (HMAF) for CCHF virus proteins were kindly provided by T. Ksiazek, Centers for Disease Control and Prevention (Atlanta, GA). The antipeptide antibody used in this study was raised in rabbits against KLH-conjugated peptide sequences present in the mature Gn (amino acids 540–551 of CCHF virus 1bAr 10200 strain: EIHGDNYGGPGD) and was done under contract with Research Genetics Inc, Huntsville, AL. NuPAGE ready-made gels (7% or 3–8%) and recommended buffers were purchased from Invitrogen.

Because the expression of CCHF virus glycoprotein required T-7 RNA polymerase to drive the T-7 promoter, vvT-7 vaccinia virus expression system was used as performed before (48). Briefly, 5×10^5 cells were seeded onto 6-well plates a day before transfection and were infected for 1 h with vaccinia virus expressing T-7 RNA polymerase. Upon removal of the virus, cells were transfected with plasmid DNA encoding the wild type CCHF virus glycoprotein or in combination with other inhibitor expressing plasmids at 1:1 or 1:4 ratio. After 12 h, cells were labeled for 30 min with [^{35}S]cysteine and chased for 3 h. While using cells stably expressing the inhibitors, we infected them with vaccinia virus and transfected with 5 μg of plasmid DNA expressing CCHF virus glycoprotein. Immunoprecipitated proteins were resolved in NuPAGE gels and proteins were visualized by autoradiography. The protein levels were quantified using a PhosphImager (ABI Prizm) using ImageQuant program. In experiments involving infection with CCHF virus, SW13 cells stably expressing α_1-PDX or RRVL^{358} were infected with CCHF virus and labeled with ^{35}S in the Biosafety Level 4 laboratory at the CDC, Atlanta. Proteins were immunoprecipitated using HMAF, resolved in 7% NuPAGE, and bands visualized by autoradiography.

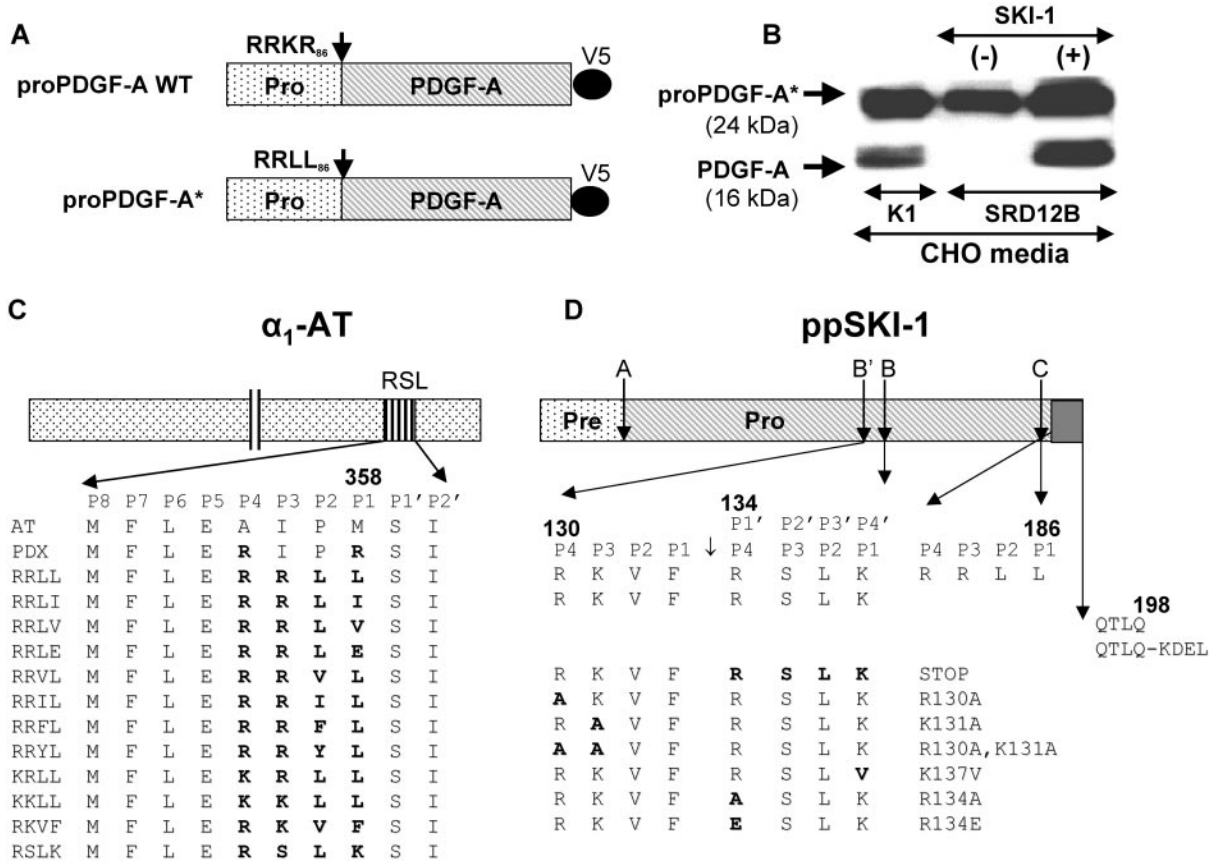

FIG. 1. **Pro-PDGF-A processing and α_1-AT/proSKI-1 mutants.** *A*, structure of pro-PDGF-A wild type and pro-PDGF-A* mutant with respective processing sites. *B*, Western blot analysis showing the processing of pro-PDGF-A* in CHO-K1 (WT), SRD-12B SKI$^{(-)}$, and SRD-12B overexpressing SKI$^{(+)}$ using a V5 mAb. *C*, schematic representation of various α_1-AT variants. The sequences of the reactive site loop (RSL) of native human α_1-AT, α_1-PDX and various α_1-AT variants are shown. *D*, schematic representation of preprosegment of the human SKI-1 (ppSKI-1). The position of the signal peptide (*Pre*) and the sequence of the B′, B, and C cleavage sites (*arrows*) in the WT or mutant prosegment are emphasized. The C-terminal of ppSKI-1 ends at amino acid 198 or with a KDEL sequence following amino acid 198.

RESULTS

Inhibition of Pro-PDGF-A (RRLL^{86}) Processing by SKI-1 in CHO-K1 Cells*—Previously (43), we had shown that SKI-1 can process intracellularly an RRLL^{86} mutant of pro-PDGF-A (pro-PDGF-A*) into PDGF-A (Fig. 1*A*), paving the way for a convenient *ex vivo* assay of SKI-1 inhibition using an anti-V5 Western blot analysis of secreted PDGF-A. The choice of CHO-K1 cells was dictated by the availability of CHO cells lacking SKI-1 (SRD-12B, called here SKI$^{(-)}$ cells) (56). In CHO-K1 cells, endogenous SKI-1 processes pro-PDGF-A*, whereas in SKI$^{(-)}$ cells such processing does not occur except in the presence of overexpressed SKI-1 (SKI$^{(+)}$) cells (Fig. 1*B*). We used this assay to test the inhibition of intracellular SKI-1 activity in CHO-K1 cells by a series of mutants of either α_1-AT (Fig. 1*C*) or the preprosegment of human SKI-1 (ppSKI-1; Fig. 1*D*).

In the α_1-AT variants, we mutated the reactive site loop sequence AIPM^{358} (P1–P4 positions) to mimic the reported SKI-1 specificity for the motif (R/K)*X*(hydrophobic)Z↓ (5–7), with a preference for the RRLL↓ cleavage site reported for the SKI-1 prosegment site C (5), and the glycoproteins of Lassa virus (44, 45) and CCHV virus (48). Co-expression of pro-PDGF-A or pro-PDGF-A* with either α_1-AT, α_1-PDX, or various serpin mutants are shown in Fig. 2. Western blots using an α_1-AT antibody revealed that α_1-AT and its mutants were expressed at similar levels (not shown). Under normal conditions, the 24-kDa pro-PDGF-A is very efficiently processed into a 16-kDa PDGF-A product. This process is completely inhibited by α_1-PDX, and most of the mutants analyzed did not have any significant inhibitory effect. However, a series of mutants RRIL^{358}, RRYL^{358}, RRVL^{358}, and RRLL^{358}, showed < 30% inhibitory effect (Fig. 2*A*, *bottom panels*). The small amount of inhibition observed might be due to the presence of a dibasic motif in the reactive site loop that may inhibit the basic convertases. In contrast, the processing of pro-PDGF-A* is inhibited by the mutants RRLL^{358}, RRVL^{358}, RRYL^{358}, RRIL^{358}, and RRLE^{358}, whereas α_1-AT, α_1-PDX and the other mutants tested were not inhibitory (Fig. 2*A*, *upper panels*). These results emphasize that serpins with a P2 hydrophobic and P4 Arg are very efficient in blocking SKI-1 activity, consistent with the SKI-1 recognition motif (5–7).

The mutations of the prosegment of SKI-1 (ppSKI-1) were selected to evaluate the importance of B/B′ primary autocatalytic zymogen processing sites (amino acids 130–137), and the segment separating the B/B′- and the C-sites. As previously reported with *in vitro* data (35), wild-type ppSKI-1 effectively inhibits the intracellular processing of pro-PDGF-A* (Fig. 2*B*, *top panels*). Retention of the prosegment in the ER through a C-terminal KDEL sequence abolished its inhibitory effect (data not shown), revealing that pro-PDGF-A* is processed at a post *cis*-Golgi compartment (57). Conversely, shortening of the prosegment to end at the C terminus of the B-site, *i.e.* at RSLK^{137} (STOP), resulted in an inactive protein. Of the B′/B mutants tested, only R130A and R134E were found to be inhibitory. Following quadruplicate independent experiments with similar results, we can state that the order of inhibitory potency of the prosegments of pro-PDGF-A* processing by SKI-1 was found to be: WT-ppSKI-1 ≈ R134E > R130A (Fig. 2*B*).

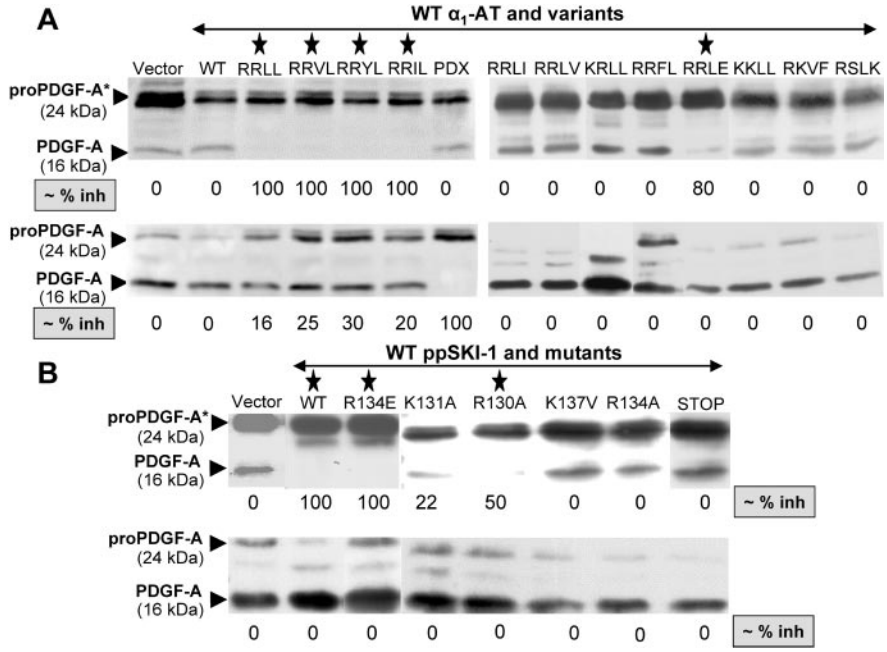

FIG. 2. **Processing of pro-PDGF-A in CHO-K1 cells.** Western blot comparing the processing of pro-PDGF-A* and pro-PDGF-A (*A*) by either vector (pIRES2-EGFP), α_1-PDX, WT-α_1-AT, various α_1-AT variants in 48-h post-transfection media, resolved by SDS-PAGE and immunoblotted using the V5 mAb. *B*, immunoblot analysis of the processing of pro-PDGF-A* and pro-PDGF-A co-transfected with ppSKI-1 mutants. The % inhibition of pro-PDGF-A or pro-PDGF-A* processing by the various α_1-AT mutants was estimated by quantitative analysis (Image Quant).

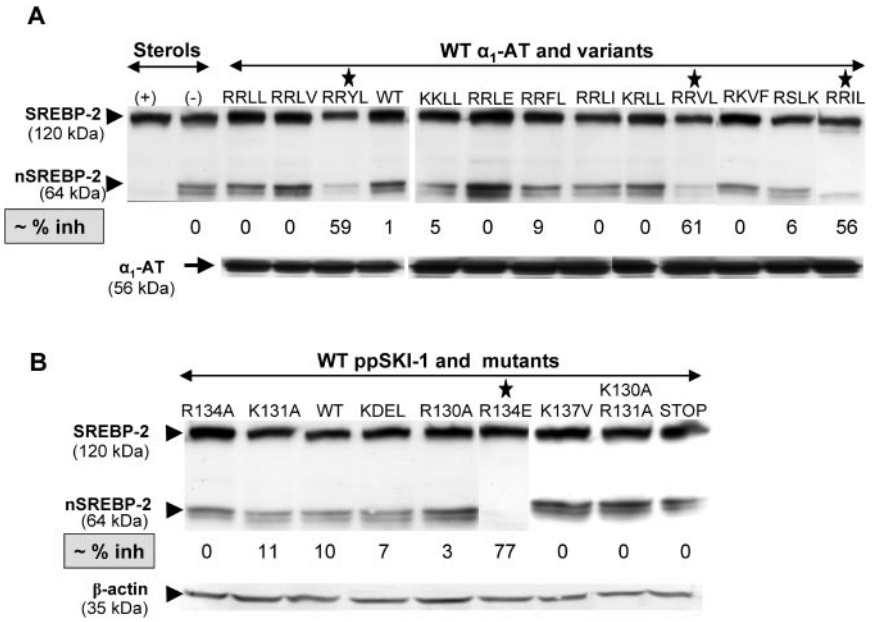

FIG. 3. **Inhibition of the processing of endogenous SREBP-2.** *A* and *B*, CHO-K1 cells were transiently transfected with the empty vector (pIRES2-EGFP), WT-α_1-AT, α_1-AT, or ppSKI-1 mutant cDNAs. 24-h post-transfection the cells were washed with PBS and incubated in (-sterol) medium for 18 h at 37 °C as described under "Experimental Procedures." Cells were lysed, and total cell extracts were resolved on 6% SDS-PAGE and endogenous hamster SREBP-2 was detected using a mouse mAb IgG-7D4 (1:200). The precursor of SREBP-2 (SREBP-2) and the nuclear processed form (nSREBP-2) migrated as doublet (56) with apparent molecular masses of ~120 kDa and ~64 kDa, respectively. *Stars* indicate significant reduction in nSREBP-2 detection, emphasizing inhibition of SKI-1 activity. *Lower panels* show immunoblot analysis of the same membrane subsequently re-hybridized with the α_1-AT antibody to confirm the level of expression (*A*) and of protein loaded based on β-actin immunoreactivity (*B*). The estimated % inhibition are shown at the *bottom* of each panel.

Inhibition of Endogenous SREBP-2 Processing by SKI-1 in CHO-K1 Cells—We next investigated the intracellular inhibitory properties of the same series of α_1-AT and ppSKI-1 mutants (Fig. 1, *C* and *D*) on the processing of endogenous proSREBP-2 (SREBP-2), a SKI-1/S1P substrate that is reported to be cleaved in the *cis*/*medial* Golgi (37). As shown in Fig. 3*A*, the membrane-bound SREBP-2 is not significantly processed into nSREBP-2 in cells incubated in medium containing cholesterol (+), whereas its characteristic doublet nuclear N-terminal fragment (nSREBP-2) is observed in the absence of exogenous sterols (−), as previously reported (56). The latter is generated by the successive cleavage of SREBP-2 by SKI-1/S1P and S2P, and requires the exit of the SREBP-2-SCAP complex from the ER to reach the Golgi, a regulated escort mechanism requiring the removal of cholesterol (49). Thus, all inhibitors were tested in the absence of exogenous sterols. Under these conditions, and in transient transfections, the α_1-AT variants that were found to be significant intracellular inhibitors (56–61% inhibition) were the RRYL^{358}, RRVL^{358}, and RRIL^{358} mutants (Fig. 3*A*). In the same vein, only the R134E mutant of ppSKI-1 was inhibitory, exhibiting ~77% inhibition (Fig. 3*B*). In all cases equal protein levels were loaded onto the gels, as evidenced by the similar amounts of immunoreactive α_1-AT (Fig. 3*A*) or β-actin (Fig. 3*B*). Thus, different from the PDGF-A* processing (Fig. 2), the SREBP-2 processing by SKI-1 is not sensitive to α_1-AT RRLL^{358}, RRLE^{358} nor to WT ppSKI-1 and its R130A mutant (Fig. 3).

Because these assays relied on the transient transfection of CHO-K1 cells with cDNAs coding for potential inhibitors of the processing of endogenous SREBP-2, and as the transfection efficacy never exceeded 70–80%, we sought to further test CHO-K1 stably expressing candidate inhibitors. In stable transfectants SREBP-2 processing was significantly inhibited by ppSKI-1 R134E (~79%) and by α_1-AT RRYL^{358} and RRVL^{358} (~65–68%) (not shown).

Inhibition of ATF6 Processing by SKI-1 in CHO-K1 Cells—We next tested the inhibitory properties of our mutants on ATF6 cleavage into its nuclear form nATF6, a processing that

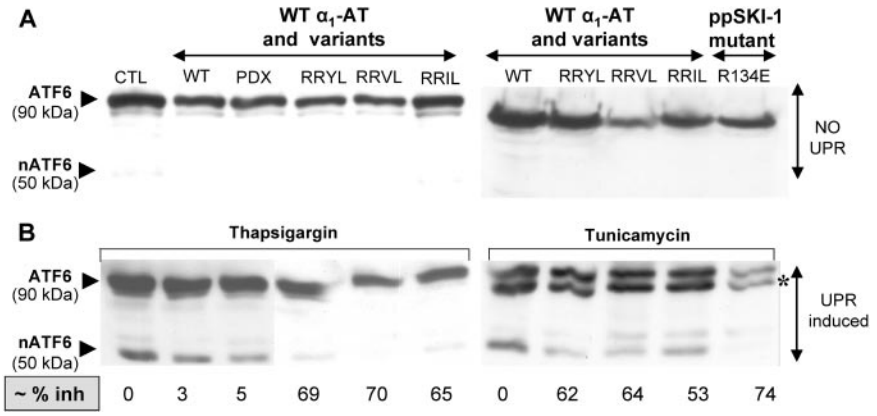

FIG. 4. **Effect of α_1-AT and proSKI-1 mutants on the processing of ER stress response factor ATF6.** Immunoblots with anti-FLAG M2 antibody showing the proteolytic processing of 3xFLAG-ATF6 in CHO-K1 cells transfected with ATF6 (CTL), α_1-AT (WT), α_1-PDX, as well as α_1-AT and proSKI-1 mutant cDNAs. The cells were either (*A*) untreated (−) or (*B*) treated (+) with 300 nM thapsigargin for 1 h or 2 μg/ml tunicamycin for 4 h. Cells were lysed and total cell extract were resolved on 6% SDS-PAGE. The estimated % inhibition is shown. The * indicates the continued presence of *N*-glycosylated ER forms after 4 h of tunicamycin inhibition (51).

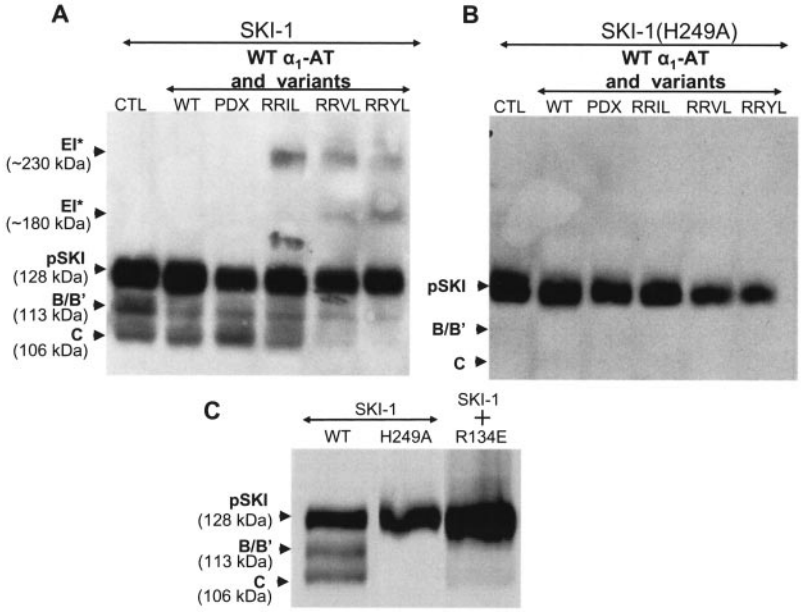

FIG. 5. **Formation of heat- and SDS-stable enzyme serpin complex.** SRD12-B (SKI$^{(-)}$) cells transiently expressing either active SKI-1-V5 (*A*) or inactive SKI-H249A-V5 (*B*) and α_1-AT (WT), α_1-PDX, α_1-AT RRIL, α_1-AT RRVL, and α_1-AT RRYL. 48-h post-transfection, cells were lysed, and total cell extract were resolved on 6% SDS-PAGE. Transferred to nitrocellulose and V5-tagged proteins detected by Western blot using a V5 mAb antibody. *C*, the effect of R134E ppSKI-1 mutant on the processing of SKI-1, its H249A mutant into the A, B′/B, and C forms.

does not require the participation of SCAP, but rather the incubation of cells under stressful conditions resulting in the activation of the UPR, such as the treatment with the Ca^{2+} ionophore thapsigargin or by the *N*-glycosylation inhibitor tunicamycin (40, 52). Under normal conditions (Fig. 4*A*, *upper panels*), in the absence or presence of the chosen inhibitors the majority of ATF6 remains in the ER as an uncleaved ~90 kDa precursor (40). However, incubation of cells with either thapsigargin or tunicamycin (Fig. 4*B*, *lower panels*) results in the generation of a ~50 kDa nATF6 (40). From the co-transfection of ATF6 and inhibitor cDNAs, it is clear that, whereas α_1-AT and α_1-PDX had no effect, the α_1-AT variants RRVL^{358}, RRYL^{358}, RRIL^{358} were relatively good inhibitors (~53–70%), and ppSKI-1 R134E (~74%) in a similar fashion to the processing of SREBP-2.

SDS-stable Complex Formation of SKI-1 with α_1-AT Variants—Serpins present a RSL that binds to the active site cleft of proteases in a substrate-like manner. The RSL is extremely flexible and assumes several different conformations, many of which are not immediately suitable for binding to the active site of the protease (58, 59). An interesting property of inhibitory serpins is their propensity to form a complex with the target proteinase (*EI**) that is resistant to heat and SDS treatment (60). The nature of the complex between the selected inhibitory α_1-AT variants and SKI-1 was examined *ex vivo*, in SKI$^{(-)}$ cells transiently overexpressing either active SKI-1 (Fig. 5*A*) or its inactive H249A mutant (Fig. 5*B*) (5), and selected α_1-AT variants. Western blot analysis of cell lysates following SDS-PAGE using a monoclonal antibody that recognizes the V5-epitope at the C terminus of active SKI-1 revealed that only the RSL mutants RRIL^{358}, RRVL^{358}, and RRYL^{358} form SDS- and heat-stable complexes with SKI-1 migrating at an apparent molecular mass of ~230 kDa (Fig. 5*A*). A minor form migrating at ~180 kDa was also observed. In contrast, neither WT-α_1-AT nor α_1-PDX form such complexes with SKI-1 (Fig. 5*A*), and none of the serpins tested can form an SDS-stable complex with inactive SKI-1 (H249A) (Fig. 5*B*). We also noted that the propeptide mutant R134E and that the RSL mutants RRVL^{358} and RRYL^{358} inhibited the formation of both the B/B′ and the active SKI-1 C-forms, suggesting that these are the best SKI-1 inhibitors (Fig. 5, *A* and *C*).

It should be noted that α_1-PDX was reported to form similar complexes with furin (22, 61), PC5, and PACE4 (27). Similar analyses were performed in HK293 cells transiently overexpressing both SKI-1 and the serpins (Fig. 6). Again, we could detect the ~230 kDa intracellular complex between SKI-1 and either α_1-AT RRYL^{358}, RRVL^{358}, and RRIL^{358}, but not with α_1-PDX or WT-α_1-AT (Fig. 6*A*). Because membrane-bound SKI-1 autocatalytically sheds itself releasing a soluble secreted form (5, 7), we also tested the media using an α_1-AT antibody and detected similar complexes (Fig. 6*B*). As a further control, we also tested whether these inhibitors can form complexes with the soluble basic-amino acid-specific PC5A (62). Although not shown, only α_1-PDX was shown to form a ~230-kDa com-

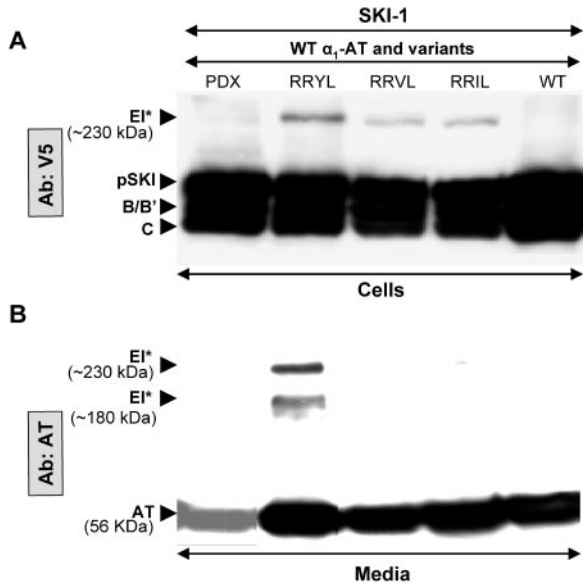

FIG. 6. **α_1-AT variants form heat- and SDS-stable complexes with SKI-1.** HK293 cells were transfected with SKI-1-V5 and α_1-AT (WT), α_1-PDX, and α_1-AT variants. Two days post-transfection, lysates and media were resolved by 6% SDS-PAGE and analyzed by Western blotting using either a V5 mAb (*A*) or an α_1-AT antibody (*B*). The *arrowhead* indicate EI*-enzyme serpin complex.

plex with PC5A, both in cells and medium.

Inhibition of the SKI-1-mediated Processing of the CCHF Virus Glycoprotein—We have previously shown that the mature Gn (~37 kDa) of CCHF virus is processed from Pre-Gn (~140 kDa) by SKI-1 following the RRLL↓ tetrapeptide sequence (amino acids 516–519). Furthermore, a CHO-K1-derived cell line expressing a mutant form of SKI-1 (7) was defective in Pre-Gn processing (48). After screening many SKI-1 inhibitors and identifying a few potent ones effective for cellular proteins (Figs. 1–6), we wanted to analyze if those inhibitors were able to reduce or block the processing of a virus glycoprotein processed by SKI-1. For that purpose, CHO-K1 cells stably expressing α_1-AT, RRVL^{358}, RRYL^{358}, or R134E were infected by vaccinia virus expressing T7 RNA polymerase and transfected with a T7 driven plasmid expressing CCHF virus glycoprotein and analyzed for the inhibition in Pre-Gn processing. In cells expressing the CCHF virus glycoprotein alone or in combination with inhibitors, Pre-Gn was synthesized as a ~140 kDa protein, which was processed to Gn during a 3-h chase period (Fig. 7). Comparison of the levels of CCHF virus Pre-Gn at the 0 and 3 h chase time points shows that ~35% of Pre-Gn is proteolytically cleaved during this time period in the control CHO-α_1-AT cells (labeled as WT). As expected, mature Gn is undetectable at the 0 time point, but accumulated in significant amounts following 3-h chase. Comparison of the levels of mature Gn accumulating 3-h postchase in the RRVL^{358}, RRYL^{358}, and R134E cells relative to the control cells, indicated levels of inhibition of ~55%, ~38 and ~70%, respectively (Fig. 7). Interestingly, these SKI-1 protease inhibitors also appeared to affect the stability of the CCHF virus Pre-Gn precursor protein. Although similar amounts of Pre-Gn are detectable in the various cells during the pulse label period, less of the protein remained detectable after 3-h chase in the RRVL^{358}, RRYL^{358}, and R134E cells relative to the control WT cells. This instability appears specific to Pre-Gn, as a panel of nonspecific proteins (indicated by *asterisk*) and cellular calreticulin remained unaffected (Fig. 7).

As CHO-K1 cells are refractory to CCHF virus infection, the experiments using the CHO derived cell lines could only be performed using transfected plasmids encoding the CCHF virus glycoproteins, which does not allow analysis of the effects of these inhibitors on virus glycoprotein processing in the context of actual virus infection. To address this issue, we attempted to develop similar stably expressing cell lines but derived from SW13 cells that are the common cell line used for CCHF virus growth and experimentation. SW13 cell lines stably expressing α_1-PDX and α_1-AT-RRVL^{358} were successfully obtained. As α_1-PDX (furin inhibitor) does not affect CCHF virus Pre-Gn processing to mature Gn (48), the α_1-PDX stably expressing cells may serve as a control for assessment of processing inhibition in α_1-AT-RRVL^{358}-expressing cells. As expected, transient expression of CCHF virus glycoprotein expressed from transfected plasmids in the α_1-PDX-expressing SW13 cells resulted in the virus Pre-Gn being processed to mature Gn (Fig. 8*A*). Comparison of the level of accumulation of mature Gn in the α_1-PDX *versus* α_1-AT-RRVL^{358} expressing cells in two independent experiments demonstrated ~65–70% inhibition of Pre-Gn processing (Fig. 8*A*). This level of inhibition is somewhat higher than that observed in the corresponding CHO-derived cells (Fig. 7).

To determine the level of inhibition of virus Pre-Gn processing seen in the context of a CCHF virus infection, the α_1-PDX and RRVL^{358} stably expressing SW13 cells were infected and the level of processing assessed (Fig. 8*B*). In CCHF virus-infected SW13-α_1-PDX cells, the virus' Pre-Gn, Pre-Gc, Gc, and nucleocapsid proteins were visualized during the 30-min pulse and Gn appeared during the 5-h chase. Similar amounts of the virus proteins were observed in the α_1-AT-RRVL^{358} expressing virus-infected cells with the exception of mature Gn, which appeared to be reduced (relative to the α_1-PDX expressing cells) by ~50–55%, when normalized to nucleoprotein content. Taken together, these data and those from the CHO-derived stably expressing cell lines strongly suggest that SKI-1 protease inhibitors may represent promising compounds for further study in the development of effective antiviral strategies for control of CCHF virus infections.

DISCUSSION

Cellular localization experiments revealed that SKI-1 is sorted to the *cis*/*medial* Golgi (5, 37, 63), suggesting that it is poised to process its cognate precursors therein, SREBPs (39), ATF6 (41), Luman (42), and proBDNF (5). Whereas the modified serpin α_1-PDX (20, 21) and the PC-prosegments (31) inhibit the basic amino acid-specific PCs within the constitutive secretory pathway, no specific-inhibitor of SKI-1 is yet known. *In vitro*, the prosegment of SKI-1 is only a modest μM inhibitor of SKI-1 activity (35). Recently, Okada *et al.* (55) reported that the general serine protease inhibitor AEBSF inhibits the SKI-1-mediated Golgi processing of both SREBP-2 and ATF6α and ATF6β.

In this work we demonstrated by four different *ex vivo* assays using pro-PDGF-A*, SREBP-2, ATF6, and Pre-Gn that the best SKI-1 inhibitors are consistently ppSKI-1 R134E and the α_1-AT variants RRVL^{358}, RRYL^{358}, and RRIL^{358}. Notably, ppSKI-1 R134A was not inhibitory, whereas the R134E mutant was the most potent SKI-1 inhibitor identified in this study. Because the B′/B sequence cleaved is RKVF↓^{134}RSLK↓ (7), the R134E mutation places a Glu at the P1′ position of the B′ site (RKVF↓E^{134}) and at the P4 position of the B-site (^{134}ESLK-) (Fig. 1). The absence of a P4 Arg should block the B-site (7, 37) but could still allow the B′ to interact with the SKI-1 catalytic pocket. It should be noted that the R134E mutant of the full-length SKI-1 is ~50% less processed into the B′/B and C forms than the wild-type sequence (7). The importance of a P1′ acidic residue for SKI-1 activity was not studied before. Interestingly, the recently described crystal structure of furin clearly suggested that a P1′ acidic residue would greatly

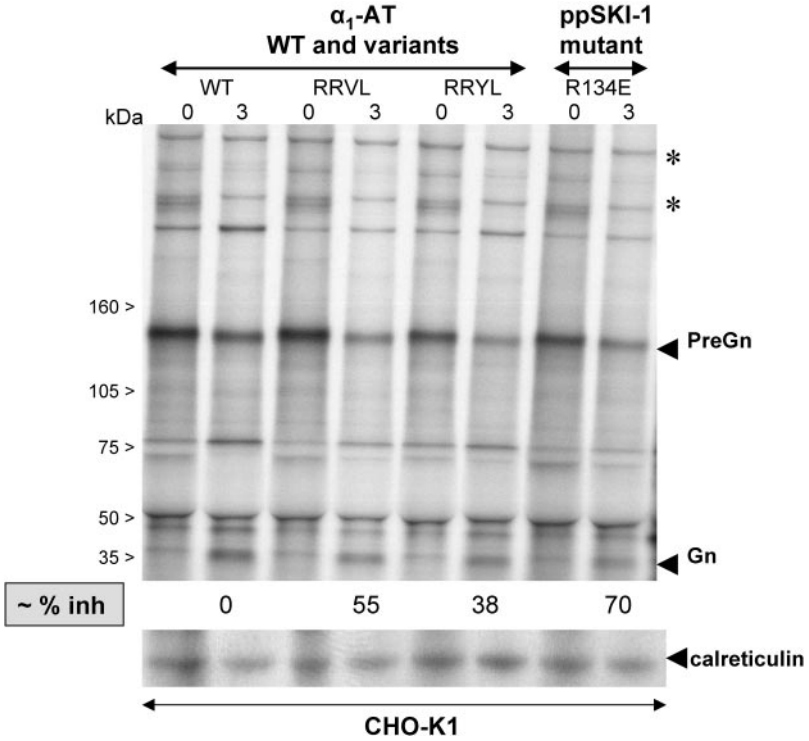

FIG. 7. **Inhibition of CCHF viral glycoprotein A.** CHO-KI-derived cells expressing α_1-AT, RRVL, RRYL, or R143E were infected with T7 expressing vaccinia virus and then transfected with a CCHF virus glycoprotein expressing plasmid. Labeled proteins were immunoprecipitated using an antipeptide antibody against CCHF virus Gn and resolved using 3–7% NuPAGE. 0 and 3 indicate the 30-min pulse and 3-h chase periods. Pre-Gn represents the precursor from which Gn (mature) is processed. The numbers at the left hand side denote the molecular weight size markers. In the *bottom*, immunoprecipitated calreticulin is provided as a loading control. The *asterisk* (*) also denotes the loading of equivalent proteins in the gel.

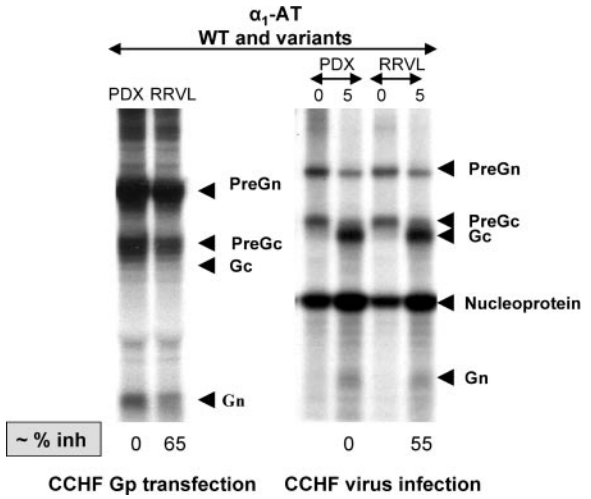

FIG. 8. **Inhibition of CCHF virus glycoprotein processing by α_1-PDX and α_1-AT RRVL variant.** SW13 cells expressing α_1-PDX and RRVL were tested for their inhibitory properties. *A*, cells were infected with vaccinia virus (10 MOI) and transfected with CCHF virus glycoprotein-expressing plasmid. CCHF Gn-specific proteins were immunoprecipitated by an antipeptide antibody and resolved in 7% NuPAGE. *B*, SW13 cells stably expressing α_1PDX or RRVL were infected with CCHF virus (CHF virus-specific) with virus adsorption for 1 h and labeling performed 18-h postinfection. Immunoprecipitation was performed using Virus HMAF and the proteins were resolved using 3–8% NuPAGE gels. Virus Pre-Gn and Pre-Gc represent the precursors of Gn and Gc, Gn and Gc are the processed forms and NP indicates the nucleocapsid protein.

favor the insertion of a substrate within the catalytic pocket (64). Indeed, a number of good furin/PC5 substrates such their own prosegments, α-integrins, and the Ebola virus glycoprotein do exhibit an acidic P1′ residue (1). Although the structure of SKI-1 is yet to be unraveled, it is tempting to speculate that similar structural constraints to those reported for furin may be applicable for SKI-1.

Our studies with the RSL mutants of α_1-AT also unraveled the selectivity of the type of P2 hydrophobic residues acceptable by SKI-1, when P1 is Leu. Thus, whereas a P2 Val, Ile, and Tyr are conducive to an inhibitory RSL, P2 Pro, Leu, Phe are not (Figs. 2–4). It may well be that the RRLL sequence that is best recognized by SKI-1 in a number of substrates (7, 44, 48) may actually be cleaved when present in the RSL of α_1-AT. Thus, whereas only an RSL with a P1 Leu in combination with either P2 Val, Ile, and Tyr resulted in an inhibitory serpin, we cannot eliminate the possibility that a P1 Val or Ile with a P2 Val, Ile, or Tyr may not also be inhibitory. This is especially true as site-directed mutagenesis studies of SREBP-2 revealed that whereas SKI-1 can cleave the WT-sequence RSVL↓ it does not process an RSVV mutant (65). However, the latter sequence may well be inhibitory.

The ability of α_1-PDX to form SDS-stable complexes with furin, PC5/6B (22, 66) and PACE4 (27), but not with PC2 (22), led to test the possibility that variants of α_1-AT that better fit the SKI-1 recognition motif may also form stable complexes with this enzyme. Indeed, our data revealed that the best inhibitors of SKI-1 activity, namely α_1-AT RRVL^{358}, RRYL^{358}, and RRIL^{358} do form such complexes with SKI-1 seen both in cells and media, whereas the non-inhibitory α_1-AT or α_1-PDX do not (Figs. 5 and 6). This observation is similar to what has already been published for α_1-PDX and furin *in vitro* (22) and in HK293 cells (27), and in all cases only a small portion of the total enzyme can be seen as a complex with the serpin on SDS-PAGE gels, suggesting that only a small amount of enzyme-serpin complex is truly resistant to SDS and heat. Thus, it is conceivable that the reactive site loop of the inhibitory α_1-AT variants exhibit typical serpin-like properties with respect to their inhibition of SKI-1.

Because SKI-1 silencing is lethal, conditional knockout experiments in liver revealed that silencing of its mRNA by ~80% results in ~50% decrease in circulating cholesterol and fatty acids (53). Therefore, the proposed R134E prosegment could conceivably represent a potentially useful inhibitor to reduce the activity of SKI-1 *in vivo*. Because the latter enzyme is also critical for the activation of some hemorrhagic fever viral surface glycoproteins (44–46, 48), we also tested our best inhibitors on the processing of Pre-Gn into Gn of CCHF virus. Unlike the other cellular proteins analyzed in this report, expression of

the glycoprotein required the need for vaccinia virus to drive the T7 promoter. Our attempts to express glycoprotein using the CMV promoter or by providing T7 RNA polymerase from a plasmid were not successful. When using vaccinia virus, we do see inhibition of Pre-Gn processing in cells expressing α_1-AT-RRVL^{358} and ppSKI-1 R134E. The fact that the Pre-Gn becomes unstable during the chase periods makes it harder to estimate the exact level of inhibition using the vaccinia system. Most of the experiments described for the inhibition of cellular proteins were performed with 1:4 substrate and inhibitor plasmid ratio. When we used that ratio in CCHF virus glycoprotein experiments, we observed a complete blockade of virus synthesis and glycoprotein stability even during the 30-min pulse period. We suggest that α_1-AT-RRVL^{358} and ppSKI-1 R134E might be good inhibitors if we could manage to get the ideal expression with improved protein stability. On the other hand, SW13-derived α_1-AT-RRVL^{358} cells showed promising inhibition (~65–70% in transfections and ~50–55% in CCHF virus infection assays) compared with α_1-PDX cells. In CCHF virus infected cells, there were no significant differences in the levels of expression of Pre-Gn, Pre-Gc, Gc, or nucleocapsid. We are in the process of developing cells stably expressing other promising inhibitors in the context of SW13 cells. Upon successful expression of all the inhibitors and necessary control, we intend to investigate the role of processing inhibition of Pre-Gn on virus assembly, release and infectivity with two target viruses (CCHF and arena viruses) which are causative agents of severe hemorrhagic manifestations in humans and whose glycoproteins are known to be activated by SKI-1. In this context, it was recently shown that lack of SKI-1-mediated processing of the glycoprotein of lymphocytic choriomeningitis virus (LCMV) leads to non-infectious virus (47). If the lack of Pre-Gn processing negatively affects the above-mentioned parameters, then the inhibitors responsible for reducing or abrogating the processing would offer a good therapeutic potential.

In conclusion, the proposed inhibitors should be very useful in defining novel functions and/or substrates of SKI-1 in cell lines of choice as well as *in vivo* in various species. They could be used as prototypes for the development highly potent small molecule SKI-1 inhibitors that could find important clinical and pharmacological applications.

Acknowledgments—We thank Dr. Ron Prywes (Columbia University, New York) for the generous gift of the 3×-FLAG-ATF6 cDNA, Dr. Joseph L. Goldstein (University of Texas, Southwestern Medical Center) for the CHO-SRD12-B cells and Dr. Gary Thomas (Vollum Institute, Portland, OR) for the α_1-AT and α_1-PDX cDNAs. We are also indebted to Eric Bergeron, Nadia Nour, Suzanne Benjannet, Marie-Claude Asselin, Louise Wickham, Josée Hamelin, Bobbie Erickson, and Annik Prat for their constant and precious advice and help. The secretarial assistance of Brigitte Mary is greatly appreciated.

REFERENCES

1. Seidah, N. G., and Chretien, M. (1999) *Brain Res.* **848,** 45–62
2. Nakayama, K. (1997) *Biochem. J.* **327,** 625–635
3. Zhou, A., Webb, G., Zhu, X., and Steiner, D. F. (1999) *J. Biol. Chem.* **274,** 20745–20748
4. Seidah, N. G. (2002) in *Co- and Post-translational Proteolysis of Proteins* (Dalbey, R. E., and Sigman, D. S., eds) Vol. XXII, pp. 237–258, Academic Press, San Diego
5. Seidah, N. G., Mowla, S. J., Hamelin, J., Mamarbachi, A. M., Benjannet, S., Toure, B. B., Basak, A., Munzer, J. S., Marcinkiewicz, J., Zhong, M., Barale, J. C., Lazure, C., Murphy, R. A., Chretien, M., and Marcinkiewicz, M. (1999) *Proc. Natl. Acad. Sci. U. S. A.* **96,** 1321–1326
6. Sakai, J., Rawson, R. B., Espenshade, P. J., Cheng, D., Seegmiller, A. C., Goldstein, J. L., and Brown, M. S. (1998) *Mol. Cell* **2,** 505–514
7. Elagoz, A., Benjannet, S., Mammarbassi, A., Wickham, L., and Seidah, N. G. (2002) *J. Biol. Chem.* **277,** 11265–11275
8. Seidah, N. G., Benjannet, S., Wickham, L., Marcinkiewicz, J., Jasmin, S. B., Stifani, S., Basak, A., Prat, A., and Chretien, M. (2003) *Proc. Natl. Acad. Sci. U. S. A.* **100,** 928–933
9. Naureckiene, S., Ma, L., Sreekumar, K., Purandare, U., Lo, C. F., Huang, Y., Chiang, L. W., Grenier, J. M., Ozenberger, B. A., Jacobsen, J. S., Kennedy, J. D., DiStefano, P. S., Wood, A., and Bingham, B. (2003) *Arch. Biochem. Biophys.* **420,** 55–67
10. Chretien, M., Mbikay, M., Gaspar, L., and Seidah, N. G. (1995) *Proc. Assoc. Am. Physicians* **107,** 47–66
11. Khatib, A. M., Siegfried, G., Chretien, M., Metrakos, P., and Seidah, N. G. (2002) *Am. J. Pathol.* **160,** 1921–1935
12. Garten, W., Hallenberger, S., Ortmann, D., Schafer, W., Vey, M., Angliker, H., Shaw, E., and Klenk, H. D. (1994) *Biochimie* (*Paris*) **76,** 217–225
13. Jean, F., Boudreault, A., Basak, A., Seidah, N. G., and Lazure, C. (1995) *J. Biol. Chem.* **270,** 19225–19231
14. Jean, F., Basak, A., DiMaio, J., Seidah, N. G., and Lazure, C. (1995) *Biochem. J.* **307,** 689–695
15. Angliker, H. (1995) *J. Med. Chem.* **38,** 4014–4018
16. Basak, A., Schmidt, C., Ismail, A. A., Seidah, N. G., Chretien, M., and Lazure, C. (1995) *Int. J. Pept. Protein Res.* **46,** 228–237
17. Cameron, A., Appel, J., Houghten, R. A., and Lindberg, I. (2000) *J. Biol. Chem.* **275,** 36741–36749
18. Basak, A., Cooper, S., Roberge, A. G., Banik, U. K., Chretien, M., and Seidah, N. G. (1999) *Biochem. J.* **338,** 107–113
19. Van Rompaey, L., Ayoubi, T., Van, D., V, and Marynen, P. (1997) *Biochem. J.* **326,** 507–514
20. Anderson, E. D., Thomas, L., Hayflick, J. S., and Thomas, G. (1993) *J. Biol. Chem.* **268,** 24887–24891
21. Benjannet, S., Savaria, D., Laslop, A., Munzer, J. S., Chretien, M., Marcinkiewicz, M., and Seidah, N. G. (1997) *J. Biol. Chem.* **272,** 26210–26218
22. Jean, F., Stella, K., Thomas, L., Liu, G., Xiang, Y., Reason, A. J., and Thomas, G. (1998) *Proc. Natl. Acad. Sci. U. S. A.* **95,** 7293–7298
23. Dahlen, J. R., Jean, F., Thomas, G., Foster, D. C., and Kisiel, W. (1998) *J. Biol. Chem.* **273,** 1851–1854
24. Lu, W., Zhang, W., Molloy, S. S., Thomas, G., Ryan, K., Chiang, Y., Anderson, S., and Laskowski, M., Jr. (1993) *J. Biol. Chem.* **268,** 14583–14585
25. Komiyama, T., and Fuller, R. S. (2000) *Biochemistry* **39,** 15156–15165
26. Komiyama, T., VanderLugt, B., Fugere, M., Day, R., Kaufman, R. J., and Fuller, R. S. (2003) *Proc. Natl. Acad. Sci. U. S. A.* **100,** 8205–8210
27. Tsuji, A., Ikoma, T., Hashimoto, E., and Matsuda, Y. (2002) *Protein Eng.* **15,** 123–130
28. Fu, X., Inouye, M., and Shinde, U. (2000) *J. Biol. Chem.* **275,** 16871–16878
29. Lesage, G., Tremblay, M., Guimond, J., and Boileau, G. (2001) *FEBS Lett.* **508,** 332–336
30. Anderson, E. D., Van Slyke, J. K., Thulin, C. D., Jean, F., and Thomas, G. (1997) *EMBO J.* **16,** 1508–1518
31. Zhong, M., Munzer, J. S., Basak, A., Benjannet, S., Mowla, S. J., Decroly, E., Chretien, M., and Seidah, N. G. (1999) *J. Biol. Chem.* **274,** 33913–33920
32. Boudreault, A., Gauthier, D., and Lazure, C. (1998) *J. Biol. Chem.* **273,** 31574–31580
33. Nour, N., Basak, A., Chretien, M., and Seidah, N. G. (2003) *J. Biol. Chem.* **278,** 2886–2895
34. Fugere, M., Limperis, P. C., Beaulieu-Audy, V., Gagnon, F., Lavigne, P., Klarskov, K., Leduc, R., and Day, R. (2002) *J. Biol. Chem.* **277,** 7648–7656
35. Toure, B. B., Munzer, J. S., Basak, A., Benjannet, S., Rochemont, J., Lazure, C., Chretien, M., and Seidah, N. G. (2000) *J. Biol. Chem.* **275,** 2349–2358
36. Benjannet, S., Elagoz, A., Wickham, L., Mamarbachi, M., Munzer, J. S., Basak, A., Lazure, C., Cromlish, J. A., Sisodia, S., Checler, F., Chretien, M., and Seidah, N. G. (2001) *J. Biol. Chem.* **276,** 10879–10887
37. Espenshade, P. J., Cheng, D., Goldstein, J. L., and Brown, M. S. (1999) *J. Biol. Chem.* **274,** 22795–22804
38. Rawson, R. B., Zelenski, N. G., Nijhawan, D., Ye, J., Sakai, J., Hasan, M. T., Chang, T. Y., Brown, M. S., and Goldstein, J. L. (1997) *Mol. Cell* **1,** 47–57
39. Brown, M. S., and Goldstein, J. L. (1999) *Proc. Natl. Acad. Sci. U. S. A.* **96,** 11041–11048
40. Kaufman, R. J. (2002) *J. Clin. Investig.* **110,** 1389–1398
41. Ye, J., Rawson, R. B., Komuro, R., Chen, X., Dave, U. P., Prywes, R., Brown, M. S., and Goldstein, J. L. (2000) *Mol. Cell* **6,** 1355–1364
42. Raggo, C., Rapin, N., Stirling, J., Gobeil, P., Smith-Windsor, E., O'Hare, P., and Misra, V. (2002) *Mol. Cell. Biol.* **22,** 5639–5649
43. Siegfried, G., Khatib, A. M., Benjannet, S., Chretien, M., and Seidah, N. G. (2003) *Cancer Res.* **63,** 1458–1463
44. Lenz, O., ter Meulen, J., Klenk, H. D., Seidah, N. G., and Garten, W. (2001) *Proc. Natl. Acad. Sci. U. S. A.* **98,** 12701–12705
45. Basak, A., Chretien, M., and Seidah, N. G. (2002) *FEBS Lett.* **514,** 333–339
46. Beyer, W. R., Popplau, D., Garten, W., Von Laer, D., and Lenz, O. (2003) *J. Virol.* **77,** 2866–2872
47. Kunz, S., Edelmann, K. H., de la Torre, J. C., Gorney, R., and Oldstone, M. B. (2003) *Virology* **314,** 168–178
48. Vincent, M. J., Sanchez, A. J., Erickson, B. R., Basak, A., Chretien, M., Seidah, N. G., and Nichol, S. T. (2003) *J. Virol.* **77,** 8640–8649
49. Yang, T., Espenshade, P. J., Wright, M. E., Yabe, D., Gong, Y., Aebersold, R., Goldstein, J. L., and Brown, M. S. (2002) *Cell* **110,** 489–500
50. Rawson, R. B. (2003) *Biochem. Soc. Symp.* 221–231
51. Haze, K., Yoshida, H., Yanagi, H., Yura, T., and Mori, K. (1999) *Mol. Biol. Cell* **10,** 3787–3799
52. Shen, J., Chen, X., Hendershot, L., and Prywes, R. (2002) *Dev. Cell* **3,** 99–111
53. Yang, J., Goldstein, J. L., Hammer, R. E., Moon, Y. A., Brown, M. S., and Horton, J. D. (2001) *Proc. Natl. Acad. Sci. U. S. A.* **98,** 13607–13612
54. Schlombs, K., Wagner, T., and Scheel, J. (2003) *Proc. Natl. Acad. Sci. U. S. A.*
55. Okada, T., Haze, K., Nadanaka, S., Yoshida, H., Seidah, N. G., Hirano, Y., Sato, R., Negishi, M., and Mori, K. (2003) *J. Biol. Chem.* **278,** 31024–31032
56. Rawson, R. B., Cheng, D., Brown, M. S., and Goldstein, J. L. (1998) *J. Biol. Chem.* **273,** 28261–28269
57. Pelham, H. R. (1988) *EMBO J.* **7,** 913–918
58. Lawrence, D. A. (1997) *Nat. Struct. Biol.* **4,** 339–341
59. Wilczynska, M., Fa, M., Karolin, J., Ohlsson, P. I., Johansson, L. B., and Ny, T. (1997) *Nat. Struct. Biol.* **4,** 354–357

60. Potempa, J., Korzus, E., and Travis, J. (1994) *J. Biol. Chem.* **269,** 15957–15960
61. Dufour, E. K., Denault, J. B., Hopkins, P. C., and Leduc, R. (1998) *FEBS Lett.* **426,** 41–46
62. Lusson, J., Vieau, D., Hamelin, J., Day, R., Chretien, M., and Seidah, N. G. (1993) *Proc. Natl. Acad. Sci. U. S. A.* **90,** 6691–6695
63. Elagoz, A., Benjannet, S., Mammarbassi, A., Wickham, L., and Seidah, N. G. (2001) *J. Biol. Chem.*
64. Henrich, S., Cameron, A., Bourenkov, G. P., Kiefersauer, R., Huber, R., Lindberg, I., Bode, W., and Than, M. E. (2003) *Nat. Struct. Biol.* **10,** 520–526
65. Duncan, E. A., Brown, M. S., Goldstein, J. L., and Sakai, J. (1997) *J. Biol. Chem.* **272,** 12778–12785
66. Dufour, E. K., Denault, J. B., Bissonnette, L., Hopkins, P. C., Lavigne, P., and Leduc, R. (2001) *J. Biol. Chem.* **276,** 38971–38979

Development of Protein-based Inhibitors of the Proprotein of Convertase SKI-1/S1P: PROCESSING OF SREBP-2, ATF6, AND A VIRAL GLYCOPROTEIN

Philomena Pullikotil, Martin Vincent, Stuart T. Nichol and Nabil G. Seidah

J. Biol. Chem. 2004, 279:17338-17347.
doi: 10.1074/jbc.M313764200 originally published online February 16, 2004
